

Bidirectional two colored light emission from stress-activated ZnS-microparticles-embedded polydimethylsiloxane elastomer films

Soon Moon Jeong,* Seongkyu Song, Kyung-Il Joo, Jaewook Jeong and Seok-Hwan Chung

Nano & Bio Research Division, Daegu Gyeongbuk Institute of Science and Technology, 50-1 Sang-Ri, Hyeonpung-Myeon, Dalseong-Gun, Daegu 711-873, Republic of Korea

*smjeong@dgist.ac.kr

Abstract: Bidirectional two-colored mechanoluminescent light emission has been demonstrated by unifying two polydimethylsiloxane elastomer layers functionalized with zinc sulfide doped with Cu (ZnS:Cu) or Cu and Mn (ZnS:Cu,Mn). The bilayered composite films are simply fabricated by dispensing uncured ZnS:Cu,Mn + PDMS onto previously spin-coated and hardened ZnS:Cu + PDMS film. The robust PDMS-PDMS bonding yields a film which can simultaneously emit light with color coordinates of (0.25, 0.56) and (0.50, 0.48), similar to the intrinsic colors of ZnS:Cu and ZnS:Cu,Mn, respectively. Composite films can emit light in upper and lower directions without fracture when it is stretched.

©2013 Optical Society of America

OCIS codes: (160.0160) Materials; (160.2540) Fluorescent and luminescent materials.

References and links

1. B. P. Chandra, *Luminescence of Solids* (Plenum, 1998), Chap. 10.
2. G. Alzetta, G. Chella, and S. Santucci, "Behaviour of light emission in mechanically excited ZnS phosphors," *Phys. Lett. A* **26**(2), 94–95 (1967).
3. N. A. Atari, "Piezoluminescence phenomenon," *Phys. Lett. A* **90**(1-2), 93–96 (1982).
4. A. J. Walton, "Triboluminescence," *Adv. Phys.* **26**(6), 887–948 (1977).
5. L. M. Sweeting, M. L. Cashel, and M. M. Rosenblatt, "Triboluminescence spectra of organic crystals are sensitive to conditions of acquisition," *J. Lumin.* **52**(5-6), 281–291 (1992).
6. Y. Kawaguchi, "Time-resolved fractoluminescence spectra of silica glass in a vacuum and nitrogen atmosphere," *Phys. Rev. B Condens. Matter* **52**(13), 9224–9228 (1995).
7. Y. Enomoto and H. Hashimoto, "Emission of charged particles from indentation fracture of rocks," *Nature* **346**(6285), 641–643 (1990).
8. N. C. Eddingsaas and K. S. Suslick, "Mechanoluminescence: Light from sonication of crystal slurries," *Nature* **444**(7116), 163 (2006).
9. C. G. Camara, J. V. Escobar, J. R. Hird, and S. J. Putterman, "Correlation between nanosecond X-ray flashes and stick-slip friction in peeling tape," *Nature* **455**(7216), 1089–1092 (2008).
10. N. Terasaki, H. Zhang, H. Yamada, and C.-N. Xu, "Mechanoluminescent light source for a fluorescent probe molecule," *Chem. Commun. (Camb.)* **47**(28), 8034–8036 (2011).
11. C.-N. Xu, T. Watanabe, M. Akiyama, and X. G. Zheng, "Artificial skin to sense mechanical stress by visible light emission," *Appl. Phys. Lett.* **74**(9), 1236–1238 (1999).
12. C.-N. Xu, H. Yamada, X. Wang, and X. G. Zheng, "Strong elasticoluminescence from monoclinic-structure SrAl₂O₄," *Appl. Phys. Lett.* **84**(16), 3040–3042 (2004).
13. J.-C. Zhang, C.-N. Xu, and Y.-Z. Long, "Elastico-mechanoluminescence in CaZr(PO₄)₂:Eu²⁺ with multiple trap levels," *Opt. Express* **21**(11), 13699–13709 (2013).
14. J.-C. Zhang, C.-N. Xu, S. Kamimura, Y. Terasawa, H. Yamada, and X. Wang, "An intense elastico-mechanoluminescence material CaZnOS:Mn²⁺ for sensing and imaging multiple mechanical stresses," *Opt. Express* **21**(11), 12976–12986 (2013).
15. C.-N. Xu, T. Watanabe, M. Akiyama, and X. G. Zheng, "Direct view of stress distribution in solid by mechanoluminescence," *Appl. Phys. Lett.* **74**(17), 2414–2416 (1999).
16. C.-N. Xu, X.-G. Zheng, M. Akiyama, K. Nonaka, and T. Watanabe, "Dynamic visualization of stress distribution by mechanoluminescence image," *Appl. Phys. Lett.* **76**(2), 179–181 (2000).
17. J. S. Kim, Y. N. Kwon, and K.-S. Sohn, "Dynamic visualization of crack propagation and bridging stress using the mechano-luminescence of SrAl₂O₄:(Eu,Dy,Nd)," *Acta Mater.* **51**(20), 6437–6442 (2003).
18. J. S. Kim, Y. N. Kwon, N. Shin, and K.-S. Sohn, "Visualization of fractures in alumina ceramics by mechanoluminescence," *Acta Mater.* **53**(16), 4337–4343 (2005).

19. J. S. Kim, Y. N. Kwon, N. Shin, and K.-S. Sohn, "Mechanoluminescent SrAl₂O₄:Eu,Dy phosphor for use in visualization of quasidynamic crack propagation," *Appl. Phys. Lett.* **90**(24), 241916 (2007).
20. S. M. Jeong, S. Song, S.-K. Lee, and B. Choi, "Mechanically driven light-generator with high durability," *Appl. Phys. Lett.* **102**(5), 051110 (2013).
21. S. M. Jeong, S. Song, S.-K. Lee, and N. Y. Ha, "Colour manipulation of mechanoluminescence from stress-activated composite films," *Adv. Mater.*, doi:10.1002/adma.201301679.
22. D. C. Duffy, J. C. McDonald, O. J. A. Schueller, and G. M. Whitesides, "Rapid prototyping of microfluidic systems in poly(dimethylsiloxane)," *Anal. Chem.* **70**(23), 4974–4984 (1998).
23. D. C. Duffy, O. J. A. Schueller, S. T. Brittain, and G. M. Whitesides, "Rapid prototyping of microfluidic switches in poly(dimethyl siloxane) and their actuation by electro-osmotic flow," *J. Micromech. Microeng.* **9**(3), 211–217 (1999).
24. M. A. Unger, H.-P. Chou, T. Thorsen, A. Scherer, and S. R. Quake, "Monolithic microfabricated valves and pumps by multilayer soft lithography," *Science* **288**(5463), 113–116 (2000).
25. K. Haubert, T. Drier, and D. Beebe, "PDMS bonding by means of a portable, low-cost corona system," *Lab Chip* **6**(12), 1548–1549 (2006).
26. H. Hillborg and U. W. Gedde, "Hydrophobicity recovery of polydimethylsiloxane after exposure to corona discharges," *Polymer (Guildf.)* **39**(10), 1991–1998 (1998).
27. H. Hillborg, J. F. Ankner, U. W. Gedde, G. D. Smith, H. K. Yasuda, and K. Wikstrom, "Crosslinked polydimethylsiloxane exposed to oxygen plasma studied by neutron reflectometry and other surface specific techniques," *Polymer (Guildf.)* **41**(18), 6851–6863 (2000).
28. M. Ouyang, C. Yuan, R. J. Muisener, A. Boulares, and J. T. Koberstein, "Conversion of some siloxane polymers to silicon oxide by UV/ozone photochemical processes," *Chem. Mater.* **12**(6), 1591–1596 (2000).
29. T. S. Phely-Bobin, R. J. Muisener, J. T. Koberstein, and F. Papadimitrakopoulos, "Preferential self-assembly of surface-modified Si/SiO_x nanoparticles on UV/ozone micropatterned poly(dimethylsiloxane) films," *Adv. Mater.* **12**(17), 1257–1261 (2000).
30. H. Hillborg, N. Tomczak, A. Oláh, H. Schönherr, and G. J. Vancso, "Nanoscale hydrophobic recovery: A chemical force microscopy study of UV/ozone-treated cross-linked poly(dimethylsiloxane)," *Langmuir* **20**(3), 785–794 (2004).
31. S. Satyanarayana, R. N. Karnik, and A. Majumdar, "Stamp-and-stick room-temperature bonding technique for microdevices," *J. Microelectromech. Syst.* **14**(2), 392–399 (2005).
32. M. A. Eddings, M. A. Johnson, and B. K. Gale, "Determining the optimal PDMS-PDMS bonding technique for microfluidic devices," *J. Micromech. Microeng.* **18**(6), 067001 (2008).

1. Introduction

Since mechanoluminescence was discovered by Francis Bacon, a variety of mechanoluminescent materials have been developed [1–19]. However, many previous instances of mechanoluminescent materials have suffered from weak and unrepeatable behavior due to the destructive nature of the process. To overcome these shortcomings, elastico-mechanoluminescent materials have been developed, which generate the luminescence during deformation of solids without fracture or tribo-reactions [10–16]. So far, many researches have been studied these phenomenon for stress sensors to visualize fractures (or crack propagation) and stress distributions [15–19]. Up to now, the brightness and the durability for sensing application have been improved, however, more increased light emission and repeatability has been required for increasing applicability in industrial use as an efficient mechanoluminescence display.

Recently, we proposed alternative approach for highly bright and durable mechanoluminescent composite films by focusing on the substance (polydimethylsiloxane, PDMS) that transfers the mechanical stress to the mechanoluminescent materials embedded inside [20]. We also demonstrated that by applying mechanical stress, a colourful patterned imaging device and white lighting source can be produced [21]. However, previously reported results are based on a unidirectional color observed from a single sample. Simultaneous bidirectional emission of independent mechanoluminescent colors from a single sample has not been achieved. If bidirectional emission can be realized, it would be useful for bidirectional mechanoluminescence display which show different images at both sides. Here, we demonstrate bidirectional, two-colored light emission from a single composite film consisting of zinc sulfide doped with Cu (ZnS:Cu) or Cu and Mn (ZnS:Cu,Mn) dispersed in a PDMS matrix. The emissions in opposite directions show clear color difference (green and orange) similar to the intrinsic wavelength according to energy levels of ZnS microparticles. This film demonstrates minimized light interference when it is stretched, which is very useful to display clear color differences in emitted light.

In order to make a unified sample emitting two different colors of light, bonding between ZnS:Cu + PDMS and ZnS:Cu,Mn + PDMS is one important factor. Bonding can be achieved by PDMS-PDMS interface bonding because mechanoluminescent particles are simply dispersed in the PDMS matrix. For homogenous bonding, a number of PDMS-PDMS interface bonding strategies have been reported. In order to increase the bond strength by activating cross-linked PDMS layers, various surface treatments have been studied such as plasma treatment [22–24], corona discharge [25–27] and UV/ozone treatment [28–30]. Partially cured or uncured PDMS has also been shown to be an effective, inexpensive method for creating homogeneous PDMS-PDMS assemblies [31,32]. Particularly, uncured PDMS adhesive provides a maximum bonding strength of approximately 671 kPa, followed by partial curing and oxygen plasma activation [32]. Here, we employed the uncured PDMS method to make robust PDMS-PDMS bonds in bilayered composite films.

2. Basic concept and Fabrication process

A schematic illustration of our approach is depicted in Fig. 1(a). By stretching bilayered composite films, two colors of mechanoluminescent light are emitted simultaneously in opposite directions, namely green and orange colored light in the upper and lower directions, respectively.

To fabricate the bilayer composite films, two layers consisting of ZnS:Cu + PDMS and ZnS:Cu,Mn + PDMS were bonded by coating previously hardened ZnS:Cu + PDMS film with uncured ZnS:Cu,Mn + PDMS. Figure 1(b) is a schematic illustration of the fabrication process of bilayer composite films. For the solutions, each type of mechanoluminescent particulate material (ZnS:Cu (GGS42) and ZnS:Cu,Mn (GGS12), purchased from Osram Sylvania Inc.) was added to PDMS (Wacker ELASTOSIL RT601) with the curing agent at a weight ratio of 9:1. The weight ratio of mechanoluminescent material and PDMS was maintained at 7:3. To control the thickness of the ZnS:Cu + PDMS layer, a solution consisting of ZnS:Cu particles mixed in uncured PDMS was dispensed onto a glass substrate and then spin-coated. After curing at 70 °C for 30 min, another solution (ZnS:Cu,Mn + uncured PDMS) was uniformly dispensed onto the cured ZnS:Cu + PDMS film. Note that the weight of the second solution is maintained during each fabrication process to sustain the thickness of ZnS:Cu,Mn + PDMS layer. After curing under the same conditions, the bilayered composite film is delaminated from the glass substrate for optical characterization during stretching.

3. Results and discussion

To confirm the adhered state of the two layers, cross-sectional optical microscopy (OM) and scanning electron microscopy (SEM) images were observed as shown in Figs. 1(c) and 1(d). The OM image from a UV-excited composite film shows the distinct features of two composite layers, each with a thickness of ~680 μm. However, the difference is ambiguous in the SEM image because both ZnS:Cu and ZnS:Cu,Mn particles have similar sizes (~25 μm). It must be noted that the interface between two composite layers was not observed, despite the fact that the curing of each layer is not performed simultaneously. Each composite appears as a continuous sample with a thickness of ~1,360 μm. This means that the two composite layers adhered well to each other and will avoid fracture when stretched.

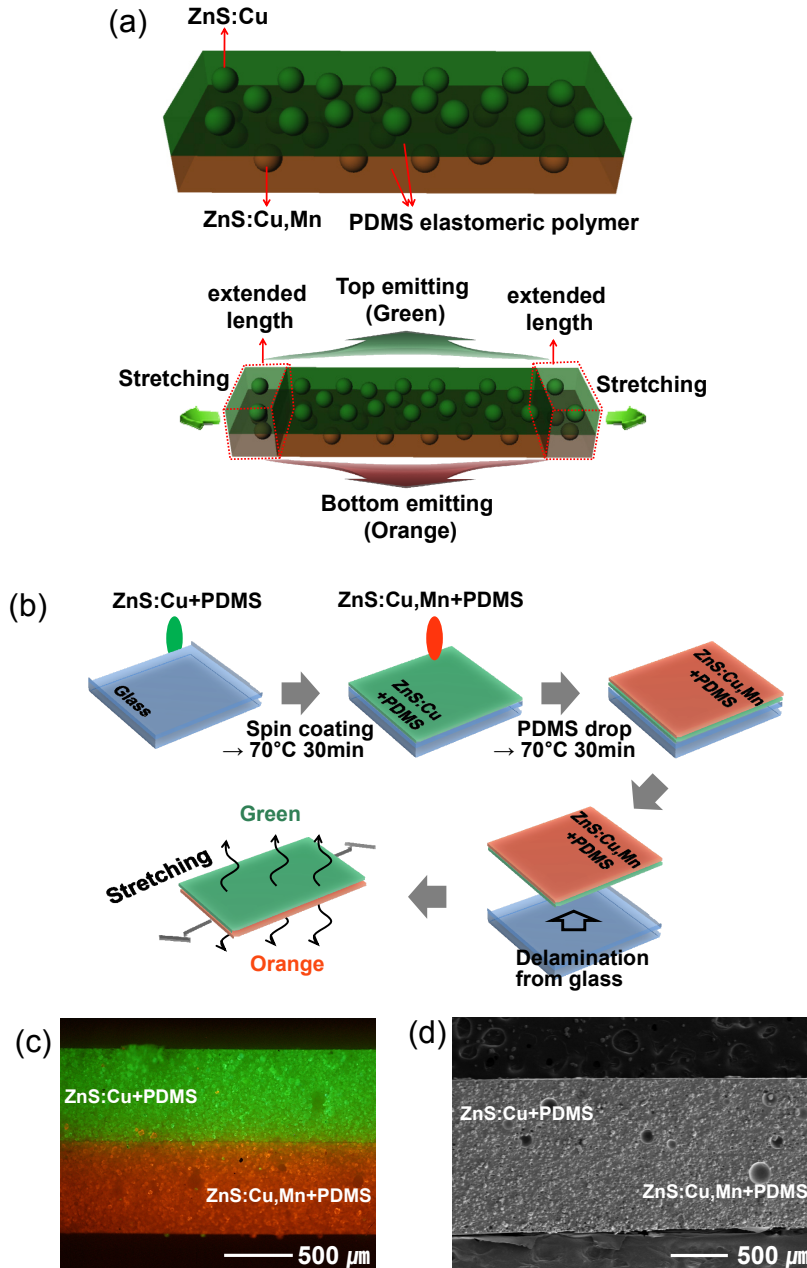


Fig. 1. (a) Schematic illustration of the approach used in this study and (b) fabrication process for bilayer composite films. (c) Cross-sectional OM and (d) SEM images observed from a bilayer composite film with total thickness of $\sim 1,360 \mu\text{m}$. Pores are observed due to bubble formation during fabrication. Note that OM image was captured from a 365-nm UV-irradiated sample to clearly show different photoluminescent features.

For characterization of mechanoluminescence of the composite films, we applied periodic stress using a stretching-releasing (S-R) system as shown in Fig. 2(a). The mechanoluminescent light was observed twice in each cycle, when the composite film was first stretched and then released (= 1 cycle). Note that we used the same S-R system as reported in ref. 20, however, unstretched sample length (see photograph in (a)) and S-R rate

were selected as 3 cm and 300 cycles per minute (cpm), respectively (previous condition: 3.5 cm, 200 cpm²⁰). The purpose of these revised conditions is to detect spectra even in the thin composite layer by increasing the emission intensity. To detect mechanoluminescent spectra from composite films during S-R cycles, a spectroradiometer (PR-655, Photo Research Inc.) with a resolution of 4 nm was suspended above the light-generating films. The detection spot size was 5.25 mm in diameter (MS-75 lens).

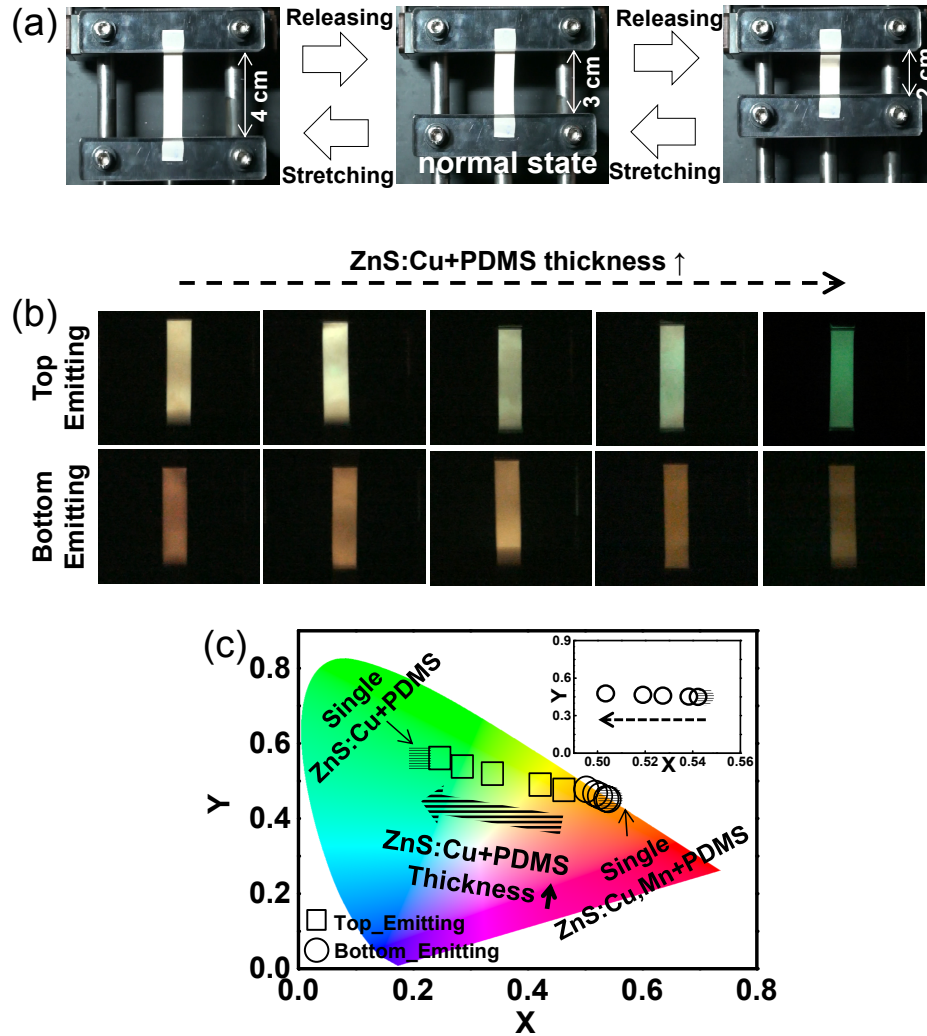


Fig. 2. Photographs of the (a) S-R system and (b) light-emitting features in the upper (upper images) and lower (lower images) directions with various ZnS:Cu + PDMS thicknesses (46 μm , 70 μm , 142 μm , 284 μm , 680 μm) during S-R motions. Note that the thickness of ZnS:Cu,Mn + PDMS is sustained at \sim 680 μm . Note that the top and bottom images shown in (b) were not taken simultaneously, because the camera was located above the composite films. In the bottom-emitting ZnS:Cu,Mn + PDMS images (lower images of (b)), photographs were taken by the same configuration after reversing the sample direction. (c) The CIE coordinate (x, y) values obtained from top- and bottom-emitting mechanoluminescence under various ZnS:Cu + PDMS thicknesses. Inset shows magnified plot of CIE coordinates of bottom-emitting light.

In order to verify the color characteristics, we took photographs of emitting mechanoluminescent composite films and measured color coordinates (Commission

Internationale de L'Eclairage, CIE), respectively. Figure 2(b) shows photographs of the top (ZnS:Cu + PDMS) and bottom (ZnS:Cu,Mn + PDMS) of mechanoluminescent composite films with various thicknesses of ZnS:Cu + PDMS composite layers under a constant stress rate applied by an S-R system operating at 300 cpm. It should be noted that the images showing the top of the film emitting light have a larger color variation, as the thickness of the ZnS:Cu + PDMS composite layer increases, whereas the color variation in the bottom layer is small. To observe the color variation more quantitatively, we also examined the color coordinates representing the colors of the top- and bottom-emitting light with various ZnS:Cu + PDMS composite layers, as shown in Fig. 2(c). For reference, the CIE coordinates of mechanoluminescent light from single layered ZnS:Cu + PDMS and ZnS:Cu,Mn + PDMS with the thickness of $\sim 700 \mu\text{m}$ were also shown. We have clearly demonstrated that the color of the top-emitting layer becomes greener (closer to ZnS:Cu) and less orange (closer to ZnS:Cu,Mn) as the thickness of ZnS:Cu + PDMS layer increases, whereas the bottom-emitting layers do not show large color variation, coinciding with photographs in Fig. 2(b).

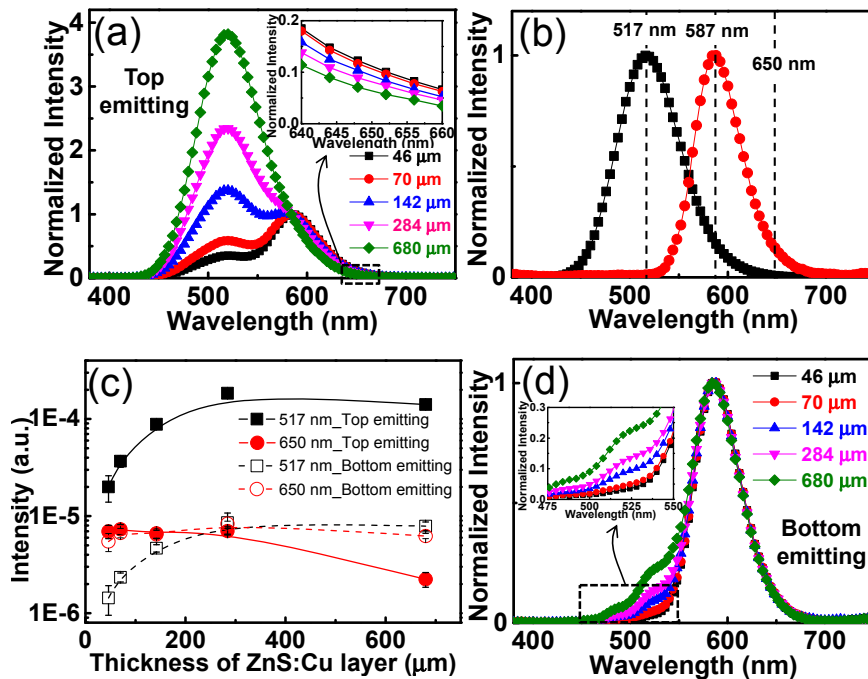


Fig. 3. Optical characteristics. (a) Normalized top-emitting mechanoluminescence spectra with reference to a wavelength of 587 nm and magnified plot (inset). (b) Normalized spectra from single ZnS:Cu + PDMS and ZnS:Cu,Mn + PDMS composite films. (c) Intensity profiles of the two selected wavelengths (517 nm and 650 nm) from top- and bottom-emitting spectra. (d) Normalized bottom-emitting mechanoluminescence spectra with reference to a wavelength of 587 nm and magnified plot (inset).

This color change can be explained by two factors simultaneously generated by stretching, namely (1) increased green light extraction, and (2) decreased orange light emission by increasing the ZnS:Cu + PDMS layer thickness. To explain these two factors using the relative intensities between two emissions, the top-emitting normalized mechanoluminescent spectra with various thicknesses of ZnS:Cu + PDMS composite layers were measured as shown in Fig. 3(a). Figure 3(b) shows two normalized mechanoluminescent spectra obtained from single layer of ZnS:Cu + PDMS and ZnS:Cu,Mn + PDMS composite films with the thickness of $\sim 700 \mu\text{m}$. The highest intensities in each spectrum are denoted as the wavelength of 517 nm and 587 nm at green and orange emission spectra, respectively. Because the

emission spectra of bilayer composite films consist of two emission spectra, color can be changed by the combination of the two spectra. It should be noted that the green emission intensity increases whereas the orange emission intensity decreases with increasing ZnS:Cu + PDMS layer thickness (Fig. 3(a)). It can be explained that the increased green light extraction is induced by the thicker emitting light source. This is supported by Fig. 3(c), showing the change in intensity profiles with the increase of ZnS:Cu + PDMS composite layer thickness. Note that we selected 650 nm as a reference for orange emission because the highest emission intensity (587 nm) involved part of green emission (Fig. 2(b)), which lead to confusion in judging a correct spectra. The intensity at 517 nm (top-emitting, closed square) increases linearly from the initial stage and becomes saturated. Whereas the emission intensity at 517 nm increases with the thickness of the ZnS:Cu + PDMS layer, emission intensity at 650 nm (top-emitting, closed circle) decreases because the orange-colored light from the ZnS:Cu + PDMS layer diminishes by scattering in the thicker ZnS:Cu + PDMS layer. This result means that the orange-colored light from the ZnS:Cu,Mn + PDMS composite layer influences the color of the top-emitting light by transmitting through the upper ZnS:Cu + PDMS layer. Because ZnS:Cu particles with an average size of $\sim 25 \mu\text{m}$ are randomly dispersed in the PDMS matrix, the amount of scattered orange light increases, which results in the decreased emission in the upper direction. Hence, the color shift of the top-emitting mechanoluminescence from (0.46, 0.48) to (0.25, 0.56) can be explained by the increase of green emission as the thickness of ZnS:Cu + PDMS layer increases (Fig. 2(c)).

On the other hand, the color variation from bottom-emitting light is relatively small compared with that of top-emitting light (lower images of Fig. 2(b)). The changes in CIE coordinates also reflect this (inset of Fig. 2(c)). Considering the previous explanation, the small color variation can be explained that most green emission diminishes by scattering in the relatively thick ZnS:Cu,Mn + PDMS layer ($\sim 680 \mu\text{m}$). Due to its similar thickness, the intensity profile at 650 nm (bottom-emitting, open circle) shows similar values, regardless of the ZnS:Cu layer thickness (Fig. 3(c)). Figure 3(d) shows bottom-emitting, normalized mechanoluminescent spectra with various thicknesses of ZnS:Cu + PDMS composite layers. The green intensities (517 nm, bottom-emitting, open square in Fig. 3c) are small, however, slightly increase with increasing ZnS:Cu + PDMS layer thickness, coinciding with small changes in CIE coordinates.

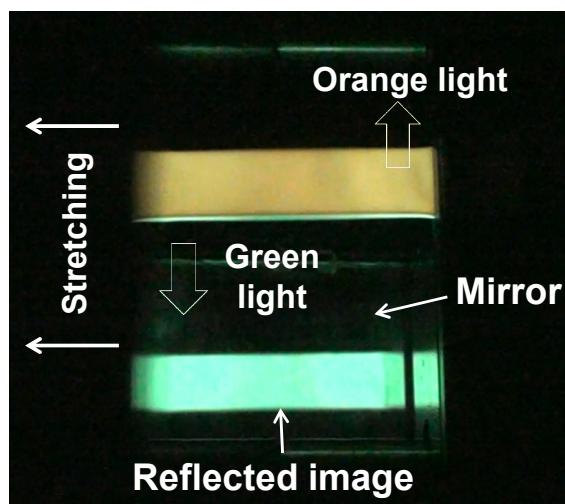


Fig. 4. Photograph of simultaneous and bidirectional two-colored light emission from a bilayer composite film during S-R motions (300 cpm).

To visually show the bidirectional two colored light from bilayer composite film with ZnS:Cu + PDMS layer thickness of $\sim 680 \mu\text{m}$ during S-R motions, we took a photograph as

shown in Fig. 4. A mirror is located under the composite film to show the orange and green colored light images simultaneously. Note that colors from top- and bottom emitting light in Fig. 4 are reversed compared with previous data because we intended that stronger green emission is proper for reflected image. The photograph clearly shows different colored light emissions. The CIE coordinate values are (0.25, 0.56) and (0.50, 0.48) for green and orange colored light, respectively, and the spectra data have been shown in Fig. 3. The colors are similar to the original colors of ZnS:Cu and ZnS:Cu,Mn indicating minimized interference.

4. Summary

In summary, bidirectional, two-colored mechanoluminescent light emission with similar CIE coordinates as pure ZnS:Cu and ZnS:Cu,Mn has been demonstrated by unifying two composite layers consisting of ZnS:Cu + PDMS and ZnS:Cu,Mn + PDMS. The bilayer composite films are simply fabricated by spin-coating uncured ZnS:Cu,Mn + PDMS onto previously hardened ZnS:Cu + PDMS films. The robust PDMS-PDMS bonding allows these composites to emit light in the upper and lower directions without fracture during stretching and releasing cycles. We expect that our light-emitting films could be applied in various industrial fields.

Acknowledgment

This work was supported by the basic research program (13-NB-02) through the Daegu Gyeongbuk Institute of Science and Technology (DGIST), funded by the Ministry of Science, ICT, and future planning of Korea.